

Supplementary Information for

Nanoscale Disintegration Kinetics of Mesoglobules in Aqueous Poly(*N*-isopropylacrylamide) Solutions Revealed by Small-Angle Neutron Scattering and Pressure Jumps

*Bart-Jan Niebuur*¹, *Leonardo Chiappisi*^{2,3}, *Florian A. Jung*¹, *Xiaohan Zhang*¹, *Alfons Schulte*^{4,*}, *Christine M. Papadakis*^{1,*}

¹Physik-Department, Fachgebiet Physik weicher Materie, Technische Universität München, James-Franck-Straße 1, 85748 Garching, Germany

²Institut Laue-Langevin, Large Scale Structures Group, 71 Avenue des Martyrs, 38042 Grenoble, France

³Technische Universität Berlin, Stranski Laboratorium für Physikalische und Theoretische Chemie, Institut für Chemie, Straße des 17. Juni 124, Sekr. TC7, D-10623 Berlin, Germany

⁴Department of Physics and College of Optics and Photonics, University of Central Florida, 4111 Libra Drive, Orlando, FL 32816-2385, U.S.A.

Comparison of Pre-jump States

Since the protocols for reaching the pre-jump conditions varied slightly for the jumps with the different jump amplitudes, we compare here the initial sample structures. The initial state was reached as follows: At 35.1 °C, the pressure was decreased from 31 MPa, which is in the one-phase region, to pressures between 0.1 and 20 MPa, which are all in the two-phase region. After an equilibration time of ~30 min, the pressure was set to 17 MPa, and the system was left to equilibrate for another 5 min.

Figure S1a shows the pre-jump scattering curves recorded prior to all 4 jumps. The scattering curves overlap rather well, which indicates that the differences in the sample history only have a minor influence on the sample structure. Fitting the scattering curves using eq 1 in the main text including the Guinier-Porod form factor and the Ornstein-Zernike structure factor results in the values of the radius of gyration of the mesoglobules, R_g , and the correlation length of concentration fluctuations, ξ_{OZ} , which are compiled in Table S1. The values are very similar to each other. Thus, the protocol for reaching the pre-jump conditions hardly influences the inner structure of the mesoglobules.

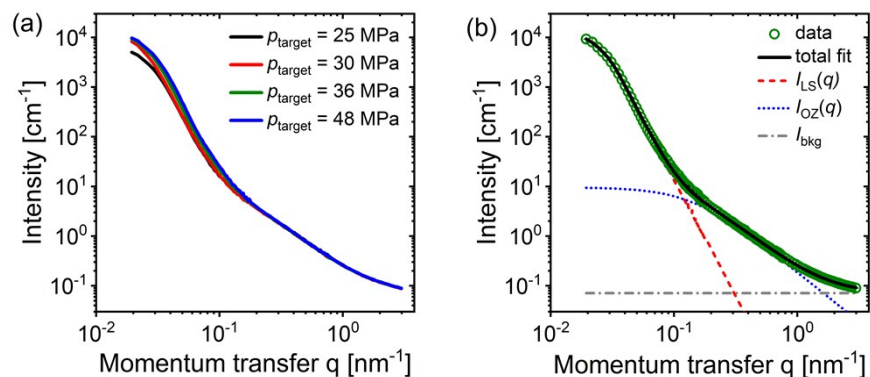


Figure S1. (a) SANS curves at 17 MPa and 35.1 °C recorded prior to the pressure jumps indicated in the graph. (b) Static SANS curve at 35.1 °C at 17 MPa before the jump to 36 MPa (olive symbols). Full line: fit of eq 1 in the main text. Broken lines: contributions to these fits: Guinier-Porod form factor (red dashed line), Ornstein-Zernike structure factor (blue dotted line), incoherent background (grey dash-dotted line).

Table S1. Structural parameters deduced from the pre-jump curves.

p_{target} (MPa)	R_g (nm)	ξ_{OZ} (nm)	m
25	72.3 ± 0.1	7.1 ± 0.1	4.6 ± 0.1
30	83.3 ± 0.1	6.7 ± 0.1	4.6 ± 0.1
36	76.6 ± 0.1	7.1 ± 0.1	4.7 ± 0.1
48	70.7 ± 0.1	6.7 ± 0.1	4.7 ± 0.1

Analysis of SANS Data

The contributions to eq 1 in the main text are the Guinier-Porod form factor, the Porod form factor and the Ornstein-Zernike structure factor. The Guinier-Porod form factor¹ reads

$$I_{LS}(q) = \begin{cases} I_G \exp\left(\frac{-q^2 R_g^2}{3}\right), & q \leq q^* \\ \frac{I_P}{q^m}, & q \geq q^* \end{cases} \quad (\text{S1})$$

R_g is the radius of gyration of the mesoglobules, m the Porod exponent, describing the surface structure of the mesoglobules, and I_G and I_P are amplitudes. At

$$q^* = \frac{1}{R_g} \sqrt{\frac{3m}{2}} \quad (\text{S2})$$

and

$$I_P = I_G \exp\left[\frac{-q^{*2} R_g^2}{3}\right] q^{*2} \quad (\text{S3})$$

the intensities as well as the slopes of the Guinier and the Porod term coincide, ensuring the continuity of both parts. The Porod exponent m is associated with the surface structure of the mesoglobules.^{2,3} The Guinier-Porod form factor was used until 3.5 s, 0.25 s, 0.3 s and 0.4 s for $p_{\text{target}} = 25, 30, 36$ and 48 MPa, respectively. Afterwards, the Porod form factor was used instead. It reads⁴

$$I_{LS}(q) = \frac{K_P}{q^m} \quad (\text{S4})$$

with K_P the Porod amplitude and m the Porod exponent.

The Ornstein-Zernike structure factor⁵ reads

$$I_{OZ}(q) = \frac{I_{OZ}}{1 + q^2 \xi_{OZ}^2} \quad (\text{S5})$$

and comprises the correlation length of concentration fluctuations, ξ_{OZ} , and an amplitude, I_{OZ} . Standard procedures were applied to account for smearing due to the divergence of the neutron beam and the wavelength distribution.⁶

Representative scattering curves along with their fits according to eq 1 in the main text are shown in Figures S2 and S3 for scattering curves measured after pressure jumps to $p_{\text{target}} = 25$ MPa and 48 MPa, respectively. Excellent agreement between the data and the fits are obtained in all cases.

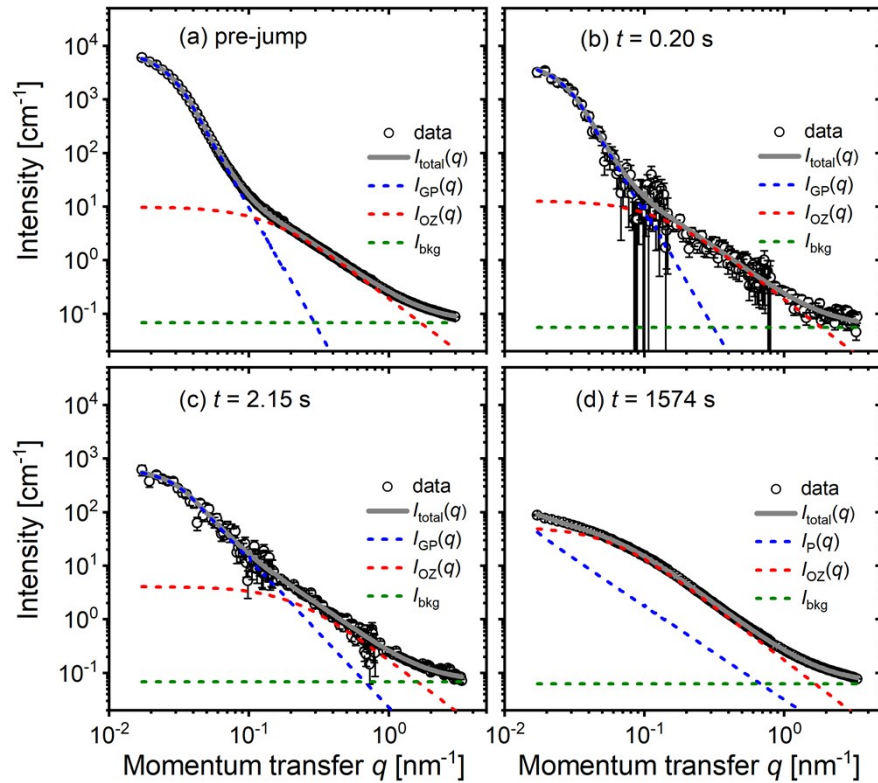


Figure S2. Representative fits of the SANS data during the pressure jump to $p_{\text{target}} = 25$ MPa obtained before the jump (a) and 0.20 s (b), 2.15 s (c) and 1574 s (d) after the jump. Grey full lines: fits of eq 1 in the main text, blue dashed lines: $I_{\text{LS}}(q)$ with the form factor used indicated in the graphs, red dashed lines: $I_{\text{OZ}}(q)$, olive dashed lines: I_{bkg} .

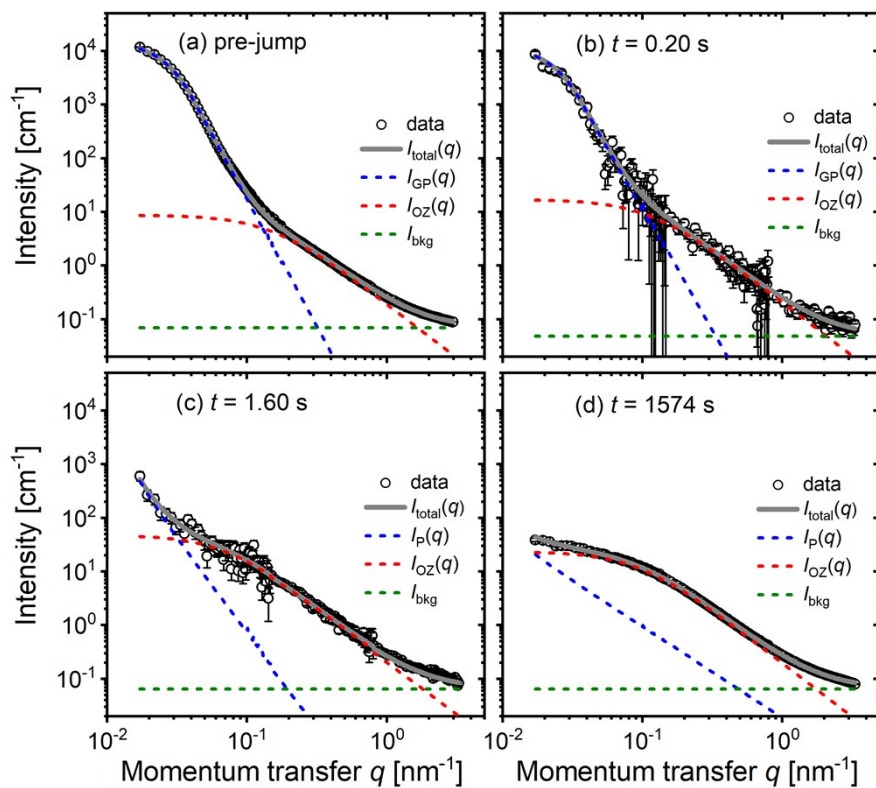


Figure S3. Representative fits of the SANS data during the pressure jump to $p_{\text{target}} = 48$ MPa obtained before the jump (a) and at 0.20 s (b), 1.60 s (c) and 1574 s (d) after the jump. Grey full lines: fits of eq 1 in the main text, blue dashed lines: $I_{\text{LS}}(q)$ with the used form factor indicated in the graphs, red dashed lines: $I_{\text{OZ}}(q)$, olive dashed lines: I_{bkg} .

Intermediate Pressure Jumps

In this section, we discuss the disintegration of mesoglobules after pressure jumps of intermediate depth. The pressure jumps were carried out as described in the main text, but with $p_{\text{target}} = 30$ and 48 MPa, respectively. Figure S4 displays the scattering curves obtained after these jumps in dependence on time. They were analysed in the same way as the data from the jumps presented in the main text.

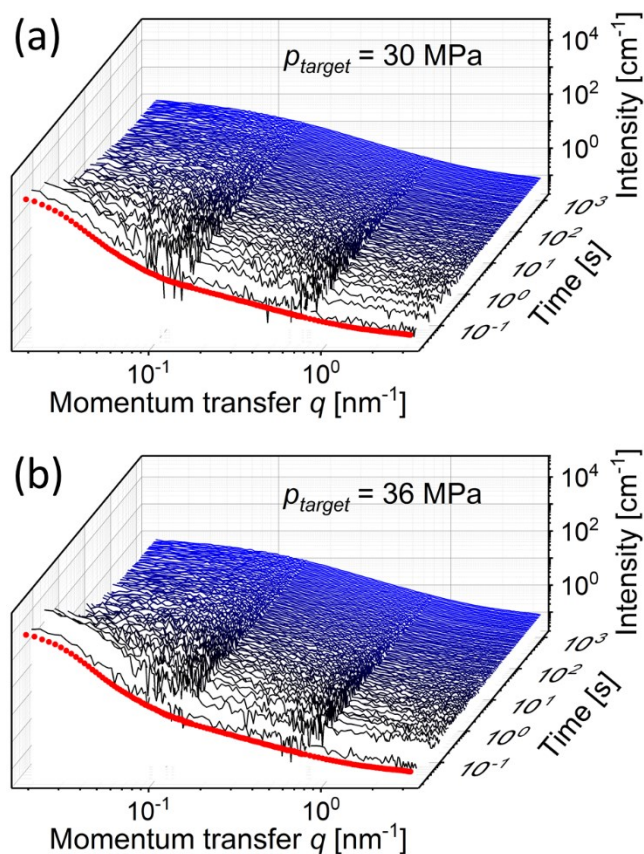


Figure S4. SANS curves of the 3 wt % PNIPAM solution in D_2O after jumps from the two-phase state to the one-phase state starting at $T = 35.1$ °C and $p_{\text{initial}} = 17$ MPa to $p_{\text{target}} = 30$ MPa (a) and $p_{\text{target}} = 36$ MPa (b) from short times (black curves) to long times (blue curves). Red symbols: pre-jump scattering curves.

The behaviour of the system after the jump with $p_{\text{target}} = 30$ MPa (Figure S5b, f and j), shows similarities with both the jumps with $p_{\text{target}} = 25$ and 48 MPa. Directly after the jump, R_g increases, i.e., the mesoglobules grow, similar to that after the jump with pressure change $p_{\text{target}} = 48$ MPa, and suggests that water diffuses into the mesoglobules, resulting in their swelling. However, this is not reflected in the evolution of ξ_{OZ} , which decreases, as for $p_{\text{target}} = 25$ MPa. Thus, the mesoglobules become more homogeneous, meaning that the chains in the interior of the mesoglobules are dissolved shortly after the jump, but these stay dense. At later times, the size of the mesoglobules cannot be resolved anymore, and the Porod approximation is used to account for scattering from the mesoglobules. Between ~ 0.5 and ~ 1 s after the jump, only the Porod approximation was sufficient to describe the system in the measured q range, i.e., no inhomogeneities at smaller length scales are observed. Afterwards, a shoulder at low q values appears, indicating the presence of structures on large length scales. ξ_{OZ} , which gives an estimate of the size of these structures, decreases until the end of the run. This behaviour is incompatible with the mechanism of mesoglobule disintegration after large jumps, where the ongoing expansion of the mesoglobules results in an increasing ξ_{OZ} . A

speculative explanation for this behaviour is that the mesoglobules disintegrate into fragments before being dissolved completely, as has been observed previously for solid dissolution.⁷

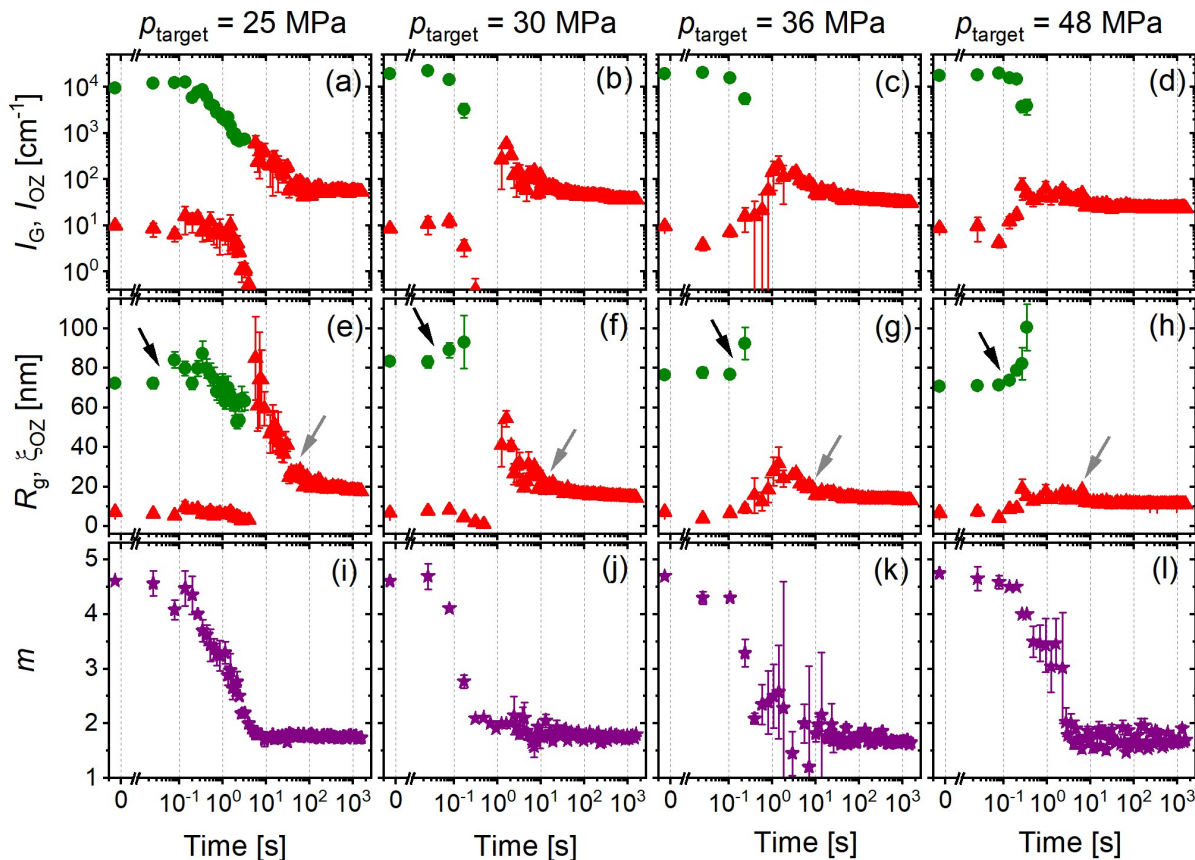


Figure S5. Time dependence of the structural parameters from fitting the SANS data for the jumps to the target pressures indicated above the graphs. (a - d): Guinier intensity I_G (green circles) and Ornstein-Zernike intensity I_{OZ} (red triangles). (e - h): Radius of gyration of the mesoglobules, R_g (green circles) and correlation length of concentration fluctuations, ξ_{OZ} (red triangles). (i - l) Porod exponent m . The black arrows mark the start of the swelling of the mesoglobules. The gray arrows mark the levelling-off of ξ_{OZ} .

The disintegration of mesoglobules after the jump with $p_{\text{target}} = 36$ MPa, shown in Figure S5c, g and k, follows qualitatively the mechanism found for $p_{\text{target}} = 48$ MPa. At ~ 0.1 s after the jump, an increase in R_g accompanied by a strong decrease in m are observed, which shows that the dense shell of the mesoglobules opens up. This allows water to enter the mesoglobules, resulting in their swelling. Simultaneously, both ξ_{OZ} and I_{OZ} increase. Thus, also in this case, chains in the interior of the mesoglobules are dissolved and diluted immediately by the water entering the mesoglobules. At later times, maxima in ξ_{OZ} as well as in I_{OZ} are observed, which are more pronounced than the ones after the jump with $p_{\text{target}} = 48$ MPa. The Ornstein-Zernike structure factor describes scattering from both concentration fluctuations in the (semi-)dilute solution and the interior of the mesoglobules; therefore, it is impossible to separate both contributions. At early times after the pressure jump, the scattering from concentration fluctuations inside the mesoglobules dominates. After the mesoglobules have disintegrated, the concentration fluctuations in the now semi-dilute solution are observed. After the jump with $p_{\text{target}} = 36$ MPa, the disintegration of the mesoglobules proceeds more slowly than after the jump with pressure change $p_{\text{target}} = 48$ MPa. Therefore, inhomogeneities in the mesoglobules may exist for longer time, leading to the observed increase of ξ_{OZ} and I_{OZ} , and therefore more pronounced maxima.

-
- (1) B. A. Hammouda, *J. Appl. Cryst.* 2010, **43**, 716.
 - (2) J. T. Koberstein, B. Morra and R. S. Stein, *J. Appl. Cryst.* 1980, **13**, 34.
 - (3) S. Ciccariello, *J. Appl. Cryst.* 1988, **21**, 117.
 - (4) G. Porod, *Kolloid Z.* 1951, **124**, 83.
 - (5) M. Shibayama, T. Tanaka and C. C. Han, *J. Chem. Phys.* 1992, **97**, 6829.
 - (6) Grillo, I. Small-Angle Neutron Scattering and Application in Soft Condensed Matter. In *Soft-Matter Characterization*; Borsali, R., Pecora, R., Eds.; Springer: Dordrecht, The Netherlands, 2008
 - (7) R. J. Seager, A. J. Acevedo, F. Spill and M. H. Zaman. *Sci. Rep.* 2018, **8**, 7711.